Multistep Production of η and Hard π^0 Mesons in Subthreshold Au-Au Collisions

A. R. Wolf,[1,*] M. Appenheimer,[1] R. Averbeck,[2] Y. Charbonnier,[3] J. Díaz,[4] A. Döppenschmidt,[5] V. Hejny,[1] S. Hlaváč,[2,†] R. Holzmann,[2] A. Kugler,[6] H. Löhner,[7] A. Marín,[4] V. Metag,[1] R. Novotny,[1] R. W. Ostendorf,[7] R. Pleskač,[6] A. Schubert,[2] Y. Schutz,[3] R. S. Simon,[2,‡] R. Stratmann,[2] H. Ströher,[1] P. Tlustý,[6] P. H. Vogt,[7] V. Wagner,[6] J. Weiß,[1] H. W. Wilschut,[7] F. Wissmann,[2] and M. Wolf[1]

[1]*II. Physikalisches Institut, Universität Gießen, D-35392 Gießen, Germany*
[2]*Gesellschaft für Schwerionenforschung, D-64291 Darmstadt, Germany*
[3]*Grand Accélérateur National d'Ions Lourds, F-14021 Caen Cedex, France*
[4]*Instituto de Física Corpuscular, Centro Mixto Universidad de Valencia–CSIC, E-46100 Burjassot, Spain*
[5]*Institut für Kernphysik, Universität Frankfurt, D-60486 Frankfurt am Main, Germany*
[6]*Nuclear Physics Institute, CZ-25068 Řež, Czech Republic*
[7]*Kernfysisch Versneller Instituut, NL-9747 AA Groningen, The Netherlands*

(Received 22 January 1998)

The neutral π^0 and η mesons are studied in ^{197}Au-^{197}Au collisions at an incident energy of 800A MeV, substantially below the threshold for η production in N-N collisions. While the gross π^0 multiplicity increases almost linearly with the number of participant nucleons, the multiplicities of η and hard π^0 mesons show a stronger than linear dependence. The nonlinearity is governed by the average transverse-mass excess $\langle m_t \rangle - (\sqrt{s} - 2m_N)$ of the mesons and is insensitive to their final-state interaction in the nuclear medium. [S0031-9007(98)06389-3]

PACS numbers: 25.75.Dw, 13.75.Cs, 25.70.Ef

Heavy-ion collisions at incident energies around 1A GeV provide a unique tool for studying nuclear matter at high density and temperature. In the course of the collision the initial kinetic energy is converted not only into compression and thermal motion but also into intrinsic excitation. A substantial fraction of the nucleons is excited to short-lived states which decay via meson emission [1,2]. Because of their higher masses these resonance states may serve as a short-term energy reservoir, facilitating the population of still heavier resonances by multistep excitation [3,4]. This mechanism makes it possible to produce mesons in collisions between heavy nuclei at beam energies below the production threshold in free N-N collisions. The signature for multistep production should be a more than linear increase of the meson multiplicity with the number of nucleons participating in the reaction.

Previous investigations of subthreshold meson production in heavy collision systems have been confined to hard pions [5,6] and the K^+ meson [7]. The present Letter extends these studies to the η meson. The reaction chosen is ^{197}Au + ^{197}Au at an incident energy of 800A MeV. In the N-N system this corresponds to an available energy for particle production of $\sqrt{s} - 2m_N = 365$ MeV, a value halfway between the π^0 and the η mass. Thus, the gross π^0 yield is essentially unaffected by energy constraints, whereas the participant nucleons in the overlap zone of the collision partners have to pool their energy to create η and hard π^0 mesons with transverse mass m_t in excess of $\sqrt{s} - 2m_N$. For a given $m_t > m_\eta$ the two mesons will have quite different transverse momenta, probing complementary regimes in their final-state interaction. The experiment was performed with the two-arm photon spectrometer (TAPS) [8] at GSI Darmstadt. Au beams from the heavy-ion synchrotron with an average intensity of 1.6×10^7 particles per spill (duration 8 s) were used, impinging on a metallic target of 200 mg/cm^2.

Designed to measure π^0 and η mesons via their decay into two photons, the TAPS spectrometer consists of 384 individual BaF_2 scintillators with separate plastic scintillators for charged-particle detection positioned in front of each BaF_2 module. In the present experiment the hexagonally shaped detector telescopes were arranged in six blocks of 64 modules each. Mounted in two towers on opposite sides of the beam under 57°, the arrays had a target distance of 140 cm and were tilted by angles of 0° and ±22° with respect to the horizontal plane containing the beam axis. In this configuration mesons emitted near midrapidity ($0.40 \leq y \leq 0.78$) were detected.

Two additional detector systems, both based on plastic scintillators, were used to measure charged particles. One, an array of 48 modules arranged in three rings around the beam tube, had a distance of 10 cm from the target and covered the polar angles from 14° to 42°. The detector registered the occurrence of target reactions and provided the time-zero signal for the events. It detected the particles emitted from the collision zone, and the multiplicity of responding modules M_{react} was a measure for the centrality of the reaction. In a separate run at low beam intensity (8×10^5 particles/spill) the reaction cross section was determined with this detector by counting the incident projectiles in an auxiliary beam monitor. Our result $\sigma_{\text{react}} = 5.9 \pm 0.5$ b is in good agreement with the cross section at 1A GeV [9], with the uncertainty coming

mainly from the extrapolation to very peripheral collisions for which the reaction counter was not fully efficient and where the nuclear reactions were masked by intense δ electrons.

The other detector was the small-angle hodoscope of the KaoS Collaboration [10]. Located 5.2 m downstream from the target, the hodoscope covered the full azimuth for polar angles between 0.7° and 10.5° with 320 detector modules. The charge of the registered particles, mostly fragments of the projectile spectator, was deduced from their energy loss and from their flight time.

The event selection trigger required hits with an energy $E \geq 15$ MeV in any two TAPS blocks for the π^0 measurement and neutral hits with $E \geq 90$ MeV, at least one in each tower, for η mesons. The neutrality condition implied that only the BaF_2 element of a given detector telescope fired. In both triggers a signal from the reaction counter was mandatory but did not introduce any additional bias on the centrality of the collision. To enhance the η content of the data sample, the π^0 trigger was downscaled by a factor of 128.

An important step in the data analysis is the separation of photons from the particle background as described in Ref. [11]. For each pair of photons in a given event the invariant mass $m_{\gamma\gamma}$ is calculated from the energies of the two photons and from the opening angle between them. The π^0 and η mesons show up as structures in the invariant-mass spectrum on top of a large combinatorial background. By an event-mixing technique [12], which accounts for the photon multiplicity of the events and which keeps track of the transverse momentum p_t of the photon pairs, this background can be reproduced and subtracted with high accuracy. The resulting meson intensities are 10 300 π^0 and 5900 η at signal-to-background ratios of 27% and 2.3%, respectively.

A similar procedure for generating background-subtracted spectra also applies for other invariant quantities besides $m_{\gamma\gamma}$. Figure 1 shows the transverse-mass distributions. These spectra are corrected for the acceptance of the spectrometer which was determined in a Monte Carlo simulation as described in Ref. [12]. For $m_t \geq m_\eta$ the π^0 and η differential cross sections have comparable magnitude and their spectral shapes are similar. A fit to the data with a distribution of the form

$$\frac{1}{m_t^2}\frac{d^2\sigma}{dm_t dy} \propto e^{-m_t/T} \quad \text{with } m_t = \sqrt{m^2 + p_t^2} \qquad (1)$$

gives inverse slope parameters $T = 71 \pm 7$ MeV and $T = 49 \pm 5$ MeV for π^0 and η mesons. In the π^0 spectrum additional intensity is observed at low m_t above the extrapolation from the high-m_t region. This part of the spectrum, which represents the bulk of the π^0 yield, is characterized by $T = 50 \pm 3$ MeV, remarkably close to the inverse slope parameter of the η spectrum. For the extrapolation to the full solid angle we assume isotropically emitting thermal sources at midrapidity ($y = 0.613$) with

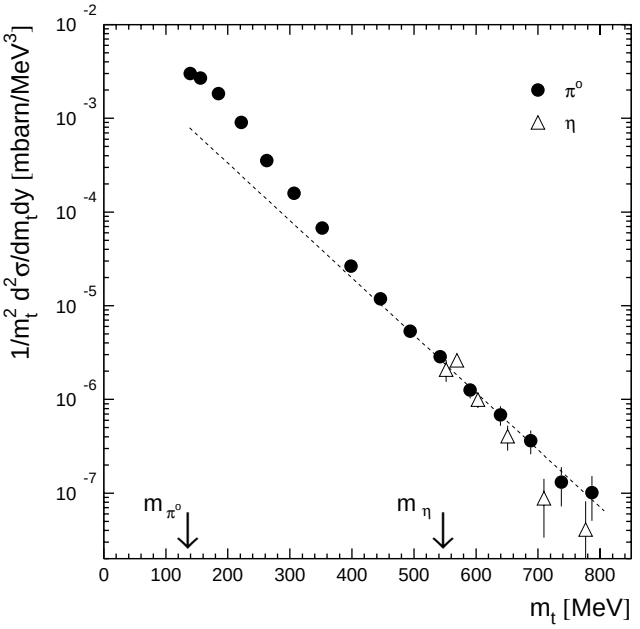

FIG. 1. Transverse-mass distributions for π^0 and η mesons. The spectra are derived from transverse-momentum spectra which were compressed to 50 MeV/c (π^0) and 100 MeV/c (η) per channel. Dashed line: fit of the distribution given by Eq. (1) to the π^0 data above m_η.

meson temperatures equal to the experimental inverse slope parameters. The meson cross sections observed in Δy and extrapolated to 4π are listed in Table I.

Using the information available from the particle detectors, the meson production can be studied as a function of the number of nucleons in the collision zone [13]. Figure 2 shows the correlation between the summed charge Z_{sum} registered in the small-angle hodoscope and the particle multiplicity M_{react} observed in the reaction counter. Ideally, in the symmetric system under study, the number of participant nucleons is given by $2A(1 - Z_{\text{sum}}/Z)$, where A and Z are the mass and charge numbers of the collision partners. In reality, however, the reaction dynamics prevents a clear-cut separation between spectators and participants. Furthermore, the limited solid angle and the marginal granularity of the particle detectors give rise to nonlinearities in the detector response.

In the analysis the multiplicity spectrum of Fig. 2 was divided into five bins, and for each bin the corresponding average value A_{part} of participant nucleons was determined together with the meson yield and the number of nuclear reactions in the target. Monte Carlo simulations with IQMD events [4] were used to correct for the nonlinearities of the detectors. Weighted by the partial reaction cross sections these A_{part} values provide the average inclusive number of participants in the Au + Au system. The result $\langle A_{\text{part}} \rangle = 125 \pm 15$ differs by less than two standard deviations from the model estimate $A/2 = 98.5$ which corresponds to the geometrical overlap of two colliding sharp spheres.

TABLE I. Average transverse masses $\langle m_t \rangle$, differential cross sections $d\sigma/dy$, and extrapolated, model-dependent total cross sections σ for π^0 and η mesons near midrapidity. Also given are the A_{part}-inclusive average meson multiplicities $\langle M \rangle = \sigma/\sigma_{\text{react}}$, the production probabilities $P = \langle M \rangle / \langle A_{\text{part}} \rangle$, and the exponents α in the power law used to describe the A_{part} dependence of the differential meson multiplicities, together with the χ^2 values of the fits.

	π^0	π^0 $(m_t \geq m_\eta)$	η
$\langle m_t \rangle$	244 ± 7 MeV	630 ± 10 MeV	610 ± 10 MeV
$d\sigma/dy$	8.5 ± 0.9 b	65 ± 8 mb	55 ± 8 mb
σ	11.8 ± 1.2 b	60 ± 7 mb	44 ± 6 mb
$\langle M \rangle$	2.0 ± 0.3	$(10.2 \pm 1.4) \times 10^{-3}$	$(7.5 \pm 1.2) \times 10^{-3}$
P	$(1.6 \pm 0.3) \times 10^{-2}$	$(8.1 \pm 1.5) \times 10^{-5}$	$(6.0 \pm 1.2) \times 10^{-5}$
α	1.2 ± 0.2, $\chi^2 = 1.1$	1.7 ± 0.2, $\chi^2 = 5.8$	

In Fig. 3 the differential meson multiplicities are given as a function of the number of nucleons participating in the collision. The m_t-inclusive gross π^0 multiplicity dM_{π^0}/dy rises almost linearly with the number of participants, in agreement with earlier observations [6,9,14]. For the η and high-m_t π^0 mesons, however, the situation is different. Here the multiplicities, jointly denoted by $dM_{m_t \geq m_\eta}/dy$, exhibit a stronger than linear dependence on A_{part}. Because of their nearly equal $\langle m_t \rangle$ and $d\sigma/dy$ (see Table I) the η and high-m_t π^0 data are considered together. Following Ref. [6], we assume a power law $dM/dy \propto A_{\text{part}}^{\alpha}$ to fit the multiplicities. The exponents α, which are listed in Table I, do confirm the qualitative trends already apparent from Fig. 3. Linear fits of dM_{π^0}/dy and $dM_{m_t \geq m_\eta}/dy$, on the other hand, give χ^2 values of 3.2 and 19.0. While a linear dependence is also acceptable for dM_{π^0}/dy, it can be rejected for $dM_{m_t \geq m_\eta}/dy$ with a confidence level of 95%.

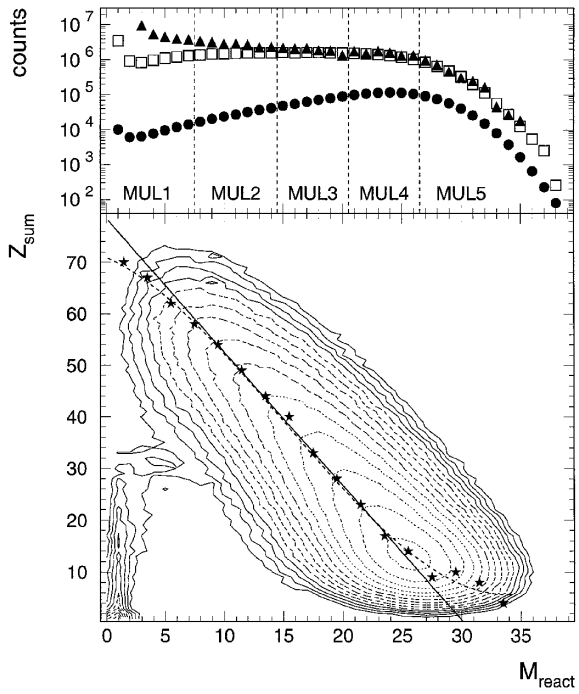

FIG. 2. Charge Z_{sum} against multiplicity M_{react}, as observed under the η trigger (lower frame). The straight line is a linear fit to the central part of the ridge, while the stars, connected by the dashed curve, represent the correlation simulated with IQMD events. The upper frame shows the projection of the two-dimensional distribution (dots), together with the five multiplicity bins used for event classification. Also shown are the multiplicity spectra for the π^0 trigger (squares) and the minimum-bias trigger (triangles), the latter requiring only a signal in the reaction counter. The partial reaction cross sections corresponding to the five multiplicity bins are 50%, 22%, 14%, 11%, and 3% of σ_{react}.

Normalization of the η and high-m_t π^0 multiplicities to the gross π^0 multiplicity gives the relative variation $dM_{m_t \geq m_\eta}/dM_{\pi^0}$ shown in Fig. 3c. These multiplicity ratios are less sensitive to systematic errors than the individual multiplicities. Fitting the power law A_{part}^{α} to $dM_{m_t \geq m_\eta}/dM_{\pi^0}$, we find $\alpha_{\text{rat}} = 0.5 \pm 0.2$ ($\chi^2 = 5.9$).

For a comparison of Au + Au with a light collision system, the TAPS results obtained for ^{40}Ar + $^{\text{nat}}$Ca at 800A MeV [15] are included in Fig. 3. The gross π^0 multiplicity in Ar + Ca depends linearly on A_{part}, but the slope is steeper than in Au + Au. The lower π^0 production probability in the heavy system, which applies over the full range of A_{part}, may to a large extent be explained by a reduction of the energy available for meson production, as more energy is converted into compression [16]. Also the η multiplicity is suppressed in Au + Au, at least in the collisions corresponding to the lower two data points in Fig. 3b which represent about 70% of σ_{react}. The enhancement observed with increasing centrality is evidence for a compensating mechanism which is insignificant for the inclusive π^0 production.

During the high-density phase of the collision, notably pions are trapped in a cyclic process of absorption and reemission which seems instrumental for subthreshold particle production [4]. Within this picture the observed nearly linear dependence of dM_{π^0}/dy on A_{part} reflects the total energy supplied by the participants, while the stronger than linear rise of $dM_{m_t \geq m_\eta}/dy$ has its origin in the extended time period over which the compression is maintained. This time period increases with

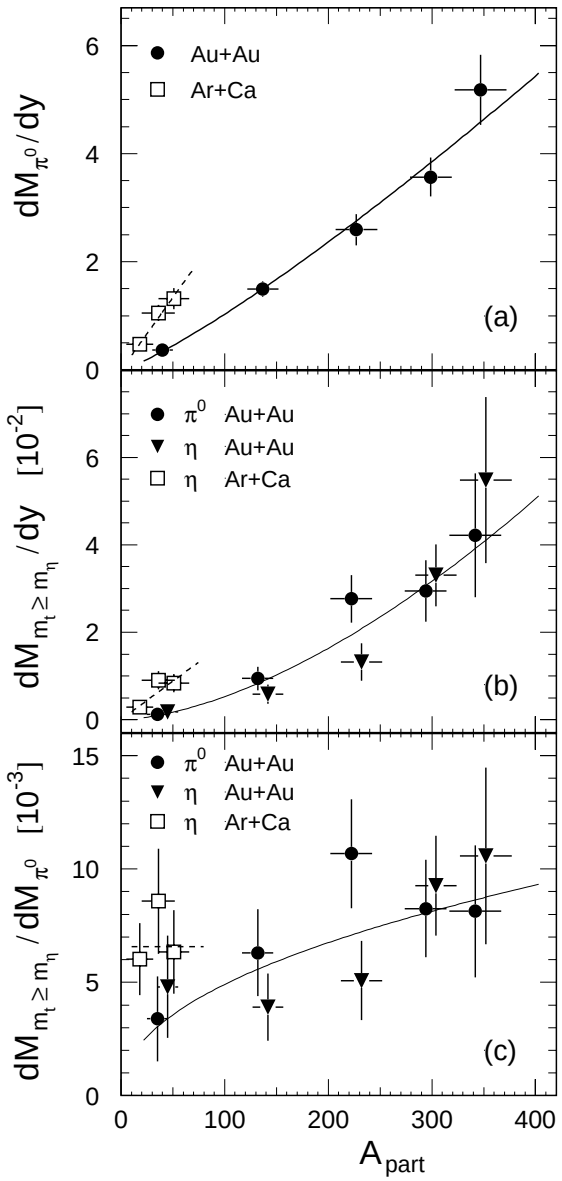

FIG. 3. Differential meson multiplicities near midrapidity as a function of the number of participants for Au + Au and Ar + Ca at 800*A* MeV. Shown are (a) the gross π^0 multiplicity dM_{π^0}/dy, (b) the multiplicities of η and high-m_t π^0 mesons, jointly denoted by $dM_{m_t \geq m_\eta}/dy$, and (c) the relative variation $dM_{m_t \geq m_\eta}/dM_{\pi^0}$. The Au + Au data are fitted by functions of the form A_{part}^{α} (solid curves), while for Ar + Ca a strictly linear dependence is indicated (dashed lines). The η and high-m_t π^0 data points in Au + Au are displaced by ± 5 units in A_{part}.

A_{part} and is long relative to the collision time of the constituents. A similar dependence of the meson multiplicity on the number of participants is known from K^+ production in Au + Au at 1*A* GeV [7]. Fitting the power law A_{part}^{α} to the differential K^+ multiplicity we find $\alpha_{K^+} = 1.6 \pm 0.3$ at an average transverse-mass excess $\langle m_t \rangle - (\sqrt{s} - m_\Lambda - m_N)$ which is about 80 MeV higher than the mass excess for the present η and high-m_t π^0 mesons (see Table I). The value for α_{K^+} is in agreement with the trend suggested by $\alpha_{m_t \geq m_\eta}$ and by previous results concerning neutral and charged pions [5,6]. The fact that hard pions, η mesons, and the antistrange K^+ experience quite different final-state interactions in the nuclear medium excludes meson absorption as a possible origin of the nonlinearity, whereas the transverse-mass excess seems to be a crucial parameter. A lowering of the K^- mass with increasing baryon density as predicted by [17] thus could lead to a measurable deviation from the common A_{part} dependence established now for pions, η, and K^+ mesons.

In summary, we have studied η and hard π^0 mesons in subthreshold ^{197}Au-^{197}Au collisions as a function of the centrality. Both the η and the high-m_t π^0 multiplicity exhibit a stronger than linear increase with the number of participant nucleons. This nonlinear A_{part} dependence, which is also found in subthreshold K^+ production, is characteristic of multistep meson production in compressed nuclear matter. It is governed by the transverse-mass excess of the produced particles and appears to be insensitive to their final-state interaction.

We thank P. Senger and the KaoS Collaboration for their help and cooperation and C. Hartnack for providing the IQMD events. This work was supported by BMBF, DAAD, DFG, and GSI (Germany), by FOM (The Netherlands), IN2P3 (France), GACR (Czech Republic), CICYT and Generalidad Valencia (Spain), and by the European Human Capital and Mobility Program.

*Present address: LH Specifications GmbH, D-63303 Dreieich–Sprendlingen, Germany.
†Permanent address: Slovak Academy of Sciences, SK-84228 Bratislava, Slovak Republic.
‡Electronic address: r.simon@gsi.de

[1] U. Mosel, Annu. Rev. Nucl. Part. Sci. **41**, 29 (1991).
[2] V. Metag, Prog. Part. Nucl. Phys. **30**, 75 (1993).
[3] Gy. Wolf, W. Cassing, and U. Mosel, Nucl. Phys. **A552**, 549 (1993).
[4] S. A. Bass *et al.*, Phys. Lett. B **335**, 289 (1994).
[5] O. Schwalb *et al.*, Phys. Lett. B **321**, 20 (1994).
[6] C. Müntz *et al.*, Z. Phys. A **357**, 399 (1997).
[7] D. Miśkowiec *et al.*, Phys. Rev. Lett. **72**, 3650 (1994).
[8] R. Novotny, IEEE Trans. Nucl. Sci. **38**, 379 (1991).
[9] D. Pelte *et al.*, Z. Phys. A **357**, 215 (1997).
[10] P. Senger *et al.*, Nucl. Instrum. Methods Phys. Res., Sect. A **327**, 393 (1993).
[11] F. M. Marqués *et al.*, Nucl. Instrum. Methods Phys. Res., Sect. A **365**, 392 (1995).
[12] R. Averbeck *et al.*, Z. Phys. A **359**, 65 (1997).
[13] W. Ahner *et al.*, Z. Phys. A **341**, 123 (1991).
[14] J. W. Harris *et al.*, Phys. Rev. Lett. **58**, 463 (1987).
[15] A. Marín *et al.*, Phys. Lett. B **409**, 77 (1997).
[16] B. Hong *et al.*, Phys. Rev. C **57**, 244 (1998).
[17] D. B. Kaplan and A. E. Nelson, Phys. Lett. B **175**, 57 (1986).